

An online optimization algorithm for the real-time quantum state tomography

Kun Zhang · Shuang Cong · Kezhi Li · Tao Wang.

Received: date / Accepted: date

Abstract Considering the presence of measurement noise in the continuous weak measurement process, the optimization problem of online quantum state tomography (QST) with corresponding constraints is formulated. Based on the online alternating direction multiplier method (OADM) and the continuous weak measurement (CWM), an online QST algorithm (QST-OADM) is designed and derived. Specifically, the online QST problem is divided into two subproblems about the quantum state and the measurement noise. The proposed algorithm adopts adaptive learning rate and reduces the computational complexity to $\mathcal{O}(d^3)$, which provides a more efficient mechanism for real-time quantum state tomography. Compared with most existing algorithms of online QST based on CWM which require time-consuming iterations in each estimation, the proposed QST-OADM can exactly solve two subproblems at each sampling. The merits of the proposed algorithm are demonstrated in the numerical experiments of online QST for 1, 2, 3, and 4-qubit systems.

Keywords Online quantum state tomography · Optimization algorithm · Online alternating direction multiplier method · Continuous weak measurement

This work was supported by the National Natural Science Foundation of China under grants no. 61720106009 and 61973290.

K. Zhang, S. Cong (*Corresponding author)
University of Science and Technology of China, Department of Automation, Hefei 230027, China
E-mail: scong@ustc.edu.cn

K. Li
University College London, 222 Euston Rd, London NW1 2DA, UK.
E-mail: ken.li@ucl.ac.uk

T. Wang
University of Science and Technology of China, Department of Automation, Hefei 230027, China

1 Introduction

Quantum state tomography (QST) is to perform $d \times d$ ($d = 2^n$) complete measurements for an n -qubit state and solve d^2 equations about the unknown state to obtain the estimated state [1–3]. Traditional quantum state tomography or estimation algorithms are offline, and the entire measurement data set is required to estimate a static fixed quantum state through multiple iterations [4,5]. The goal of the online QST is to obtain the dynamic quantum state in real-time and to be used in the quantum state feedback control system. So the online QST algorithm focuses on processing only a fraction of the available measurement data in each sampling and calculation. Such method has been used for online learning [6,7]. The state of an n -qubit system can usually be described by a density matrix $\rho \in \mathbb{C}^{d \times d}$, which satisfies the physical constraints of positive semidefinite and unit-trace Hermitian [8]. Different with the commonly used methods of QST based on projective and destructive measurements [9,10], the continuous weak measurement (CWM) proposed by Silberfarb provides a new approach to estimate quantum states [11]. Based on CWM, it is possible to gain the measurement information regarding the state to be estimated without being disturbed substantially in the measurement process, and the quantum state can be recovered from computing the ensemble averaging [12]. Due to the non-complete destructive characteristic of CWM, the online dynamic QST becomes possible.

In the online fixed state estimation of a quantum system based on CWM, people usually estimate the static initial quantum state in Heisenberg's picture, while the dynamic state can be obtained by evolutionary model [11,12,14,15]. Youssry et al. [13] proposed an online learning algorithm based on matrix exponentiated gradient method (MEG). Silberfarb et al. firstly used the maximum likelihood method (ML) to develop an online ML-estimator [11,12]. The ML-estimator satisfies the physical constraints by simply setting the negative eigenvalue of the estimated state to zero and trace normalization. However, these operations cannot guarantee the optimality of the estimated state. Ralph et al. derived the full Bayesian estimation equations for frequency tracking and parameter estimation of a single qubit system [14]. More recently, Yang et al. designed an online processing model of a two-level quantum system based on constrained least squares estimation (LS) [15,16], which was solved by the convex optimization toolbox (CVX) in MATLAB [17]. Sajede et al. extended Yang's model to an n -qubit stochastic quantum system [18]. However, considering the real-time application of QST, the currently sampled dynamic quantum state is expected to be reconstructed instantly. Moreover, the ML [12], Bayesian estimation [14] and LS solved by the CVX toolbox [15] methods are essentially batch algorithms. Although any batch algorithm can run on the state estimation problem at each sampling time to create an online estimator, this approach requires a high computational overhead. In other words, the online estimation process is a double-loop algorithm [19]. That is to run the optimization problem online in the outer loop and perform the multiple iterations in the inner loop, which becomes a much time-consuming work. Therefore, the task of real-time reconstruction for the dynamic quantum state is challenging. Because in each weak measurement sampling, only one noisy measurement value can be obtained. Meanwhile, the online algorithm only performs one iteration for each estimation, and the estimated density matrix has to meet the quantum state

constraints. In order to solve this problem and estimate the real-time quantum state effectively at each sampling time, we study the online optimization algorithm for the real-time QST.

The contribution of this paper is that a novel online QST algorithm with adaptive learning rate to reconstruct the dynamic quantum state from the noisy measurements by using the online alternating direction multiplier method (OADM) [20], called QST-OADM, is proposed. The convex optimization problem of QST with quantum state constraints is divided into two subproblems, one is the minimization of the Bregman divergence term with physical constraints for estimating the dynamic quantum state ρ_k , and the other is the minimization of an l_2 norm for estimating the measurement noise e_k . By defining an appropriate Bregman divergence term, the proposed QST-OADM algorithm can simultaneously estimate the quantum state ρ_k and measurement noise e_k at each estimation. We use the first-order information of the quantum state optimization problem, and the learning rate can be adaptively adjusted at every estimation, which can achieve more efficient state estimation. The computational complexity of LS is $\mathcal{O}(d^6)$, and the computational complexity of ML is $\mathcal{O}(d^4)$, the main computational complexity of proposed QST-OADM is $\mathcal{O}(d^3)$. The computational complexity of MEG is also $\mathcal{O}(d^3)$. The main difference between QST-OADM and MEG is that the learning rate of QST-OADM can be adjusted adaptively and the online processing framework OADM is used. In numerical experiments, our proposed algorithm is used to estimate the dynamic density matrices in 1, 2, 3, and 4-qubit systems, respectively. The experimental results are compared with other existing online algorithms.

The rest of this paper is organized as follows. N -qubit online QST based on CWM is introduced in **Section 2**. The QST-OADM algorithm is proposed in **Section 3** for solving the optimization problem of online QST with measurement noise. Numerical experiments are carried out in **Section 4**. Finally, a conclusion is drawn in **Section 5**.

2 N -qubit Online QST Based on CWM

An open n -qubit system can be described by the continuous stochastic master equation in Schrödinger picture as [9]:

$$\begin{aligned} \rho(t + \Delta t) - \rho(t) = & -\frac{i}{\hbar} [H, \rho(t)] \Delta t \\ & + \sum [L\rho(t)L^\dagger - \frac{1}{2} (L^\dagger L\rho(t) + \rho(t)L^\dagger L)] \Delta t \\ & + \sqrt{\eta} \sum [L\rho(t) + \rho(t)L^\dagger] dW, \end{aligned} \quad (1)$$

where $\rho(t) \in \mathbb{C}^{d \times d}$ denotes the quantum state density matrix; $H \in \mathbb{C}^{d \times d}$ is the Hamiltonian representing the total energy of the system; L is a bounded operator pertaining to the Lindblad interaction; L^\dagger denotes the conjugate transposition of L ; Δt is the weak measurement time; \hbar is set to 1; η is the measure efficiency; dW denotes the noise produced by measurement output for zero error measurement and satisfies $E(dW) = 0$, $E[(dW)^2] = \Delta t$; the last two terms of (1) represent the dissipation and backaction introduced by the measurement process.

The online estimation process of QST is shown in Fig.1, which is composed of the process of CWM (the left part of Fig.1) and the online QST algorithm (the right

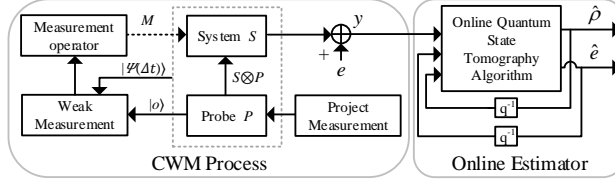


Fig. 1 Online QST estimation process.

part of Fig.1). Next, we describe the online QST estimation process according to the left and right parts of Fig.1.

1) left part: *Firstly*, as shown by the dashed box inside the left part, in the weak measurement of a single qubit system, a two-level detection system P is introduced and coupled with the estimated system S to form a joint system $S \otimes P$. Since the interaction in the weak measurement is very small, the coupled system can be considered a closed system. Therefore, the state evolution equation of the joint system is $|\Psi(\Delta t)\rangle = U(\Delta t)(|\phi\rangle \otimes |\varphi\rangle)$, where $|\phi\rangle$ and $|\varphi\rangle$ are the initial states of system P and S , respectively; $U(\Delta t) := \exp(-i\xi H \Delta t)$ is the joint evolution operator, in which $\xi > 0$ is the interaction strength of the system; $H = H_P \otimes H_S$ is the Hamiltonian of the joint system; H_P and H_S are the Hamiltonian of system P and S , respectively. *Secondly*, as shown by the arrow in the projection measurement box, through the projective measurement on the detection system P at time Δt , we can obtain the eigenstate $|o\rangle$ of the System P . *Thirdly*, as shown by the weak measurement box, we can combine the state $|\Psi(\Delta t)\rangle$ of the joint system before and after weak measurement, the output $|o\rangle$ of the System P , and the second-order Taylor expansion of the evolution equation $U(\Delta t)$ to derive the weak measurement operators $m_0(\Delta t)$ and $m_1(\Delta t)$ [16]. *Fourth*, as shown by the measurement operator box, based on the constructed weak measurement operators, we can obtain the measurement operator M indirectly acting on the estimated system S (as shown by the dotted arrow) during the continuous measurement process and the output value y with noise e . While the weak measurement operators of the n -qubit system can be calculated by the weak measurement operators of the two-level quantum system [18].

2) right part: *Firstly*, as shown by the three input arrows of the online QST algorithm, they are the noisy measurement value y obtained at each time Δt , and the previous estimates (q^{-1} represents unit delay operator), respectively. *Secondly*, as shown by the two output arrows of the online QST algorithm, the online estimator is expected to simultaneously reconstruct the current quantum state $\hat{\rho}$ and measurement noise \hat{e} to track the dynamic state. The goal of the proposed online algorithm is twofold: to obtain estimates $\hat{\rho}$ that feature *a)* high accuracy, and *b)* low computational time-consuming, so that it may serve as an effective online tracking mechanism for real-time applications.

For a two-level quantum system, its weak measurement operators are $m_0(\Delta t) := I - (L_1^\dagger L_1 / 2 + iH_1) \Delta t$ and $m_1(\Delta t) := L_1 \sqrt{\Delta t}$ [16], where we can select:

$$L_1 = \xi \sigma, H_1 = H_0 + u_x H_x, \quad (2)$$

in which σ denotes the Pauli matrix which can be one of $\{\sigma_x, \sigma_y, \sigma_z, I\}$, with $\sigma_x = \begin{pmatrix} 0 & 1 \\ 1 & 0 \end{pmatrix}$, $\sigma_y = \begin{pmatrix} 0 & -i \\ i & 0 \end{pmatrix}$, $\sigma_z = \begin{pmatrix} 1 & 0 \\ 0 & -1 \end{pmatrix}$, and I is the 2×2 identity matrix; H_0 is the free Hamiltonian, u_x is the external regulate value, and H_x is the control Hamiltonian (The choice of H_x is related to the direction in which the control is tried to be added. We select $H_x = \sigma_x$ in the experiments.). The weak measurement operators of an n -qubit system can be calculated from the tensor product of $m_0(\Delta t)$ and $m_1(\Delta t)$ as:

$$\begin{aligned} M_1(\Delta t) &= \underbrace{m_0(\Delta t) \otimes \dots \otimes m_0(\Delta t)}_n \otimes m_0(\Delta t), \\ M_2(\Delta t) &= \underbrace{m_0(\Delta t) \otimes \dots \otimes m_0(\Delta t)}_n \otimes m_1(\Delta t), \\ &\vdots \\ M_{2^n}(\Delta t) &= \underbrace{m_1(\Delta t) \otimes \dots \otimes m_1(\Delta t)}_n. \end{aligned} \quad (3)$$

Considering the weak measurement efficiency and back action in the stochastic open quantum system, the evolution operators of a two-level quantum system can be formulated as: $a_0(\Delta t) = m_0(\Delta t) + \sqrt{\eta}L_1 \cdot dW$ and $a_1(\Delta t) = m_1(\Delta t) + \sqrt{\eta}L_1 \cdot dW$ [16]. Similarly, the evolution operators of an n -qubit system can be calculated by the tensor product of $a_0(\Delta t)$ and $a_1(\Delta t)$ as:

$$\begin{aligned} A_1(\Delta t) &= \underbrace{a_0(\Delta t) \otimes \dots \otimes a_0(\Delta t)}_n \otimes a_0(\Delta t), \\ A_2(\Delta t) &= \underbrace{a_0(\Delta t) \otimes \dots \otimes a_0(\Delta t)}_n \otimes a_1(\Delta t), \\ &\vdots \\ A_{2^n}(\Delta t) &= \underbrace{a_1(\Delta t) \otimes \dots \otimes a_1(\Delta t)}_n. \end{aligned} \quad (4)$$

Based on the stochastic master equation (1) and the evolution operator (4), by taking $t = \Delta t \cdot k$, the dynamic discrete evolution model of the estimated system S can be obtained as [18]:

$$\rho_{k+1} = \sum_{i=1}^{2^n} A_i(\Delta t) \rho_k A_i(\Delta t)^\dagger, \quad (5)$$

where $k = 1, 2, \dots, N$ represents the sampling times.

The corresponding dynamic discrete measurement operators indirectly acting on the estimated system S in the CWM process is [18]:

$$M_{k+1} = \sum_{i=1}^{2^n} M_i(\Delta t) M_k M_i(\Delta t)^\dagger. \quad (6)$$

In Schrödinger picture, the measurement value of the system S at each sampling time is the initial measurement operator M_1 acting on the dynamic quantum states $\{\rho_i\}_{i=1}^k$ as:

$$y_i = \text{tr}(M_1^\dagger \rho_i) = \text{vec}(M_1)^\dagger \text{vec}(\rho_i), i = 1, 2, \dots, k, \quad (7)$$

Table 1 The Construction Process of Measurement Record Sequence.

	y_1	y_2	y_3	...	y_k
b_1	$\text{tr}(M_1^\dagger \rho_1)$				
b_2	$\text{tr}(M_2^\dagger \rho_2)$	$\text{tr}(M_1^\dagger \rho_2)$			
b_3	$\text{tr}(M_3^\dagger \rho_3)$	$\text{tr}(M_2^\dagger \rho_3)$	$\text{tr}(M_1^\dagger \rho_3)$		
\vdots	\vdots	\vdots	\vdots		
b_k	$\text{tr}(M_k^\dagger \rho_k)$	$\text{tr}(M_{k-1}^\dagger \rho_k)$	$\text{tr}(M_{k-2}^\dagger \rho_k)$...	$\text{tr}(M_1^\dagger \rho_k)$

Since a general density matrix ρ_k on n -qubits is defined through $d^2 = 4^n$ parameters, any estimation protocol may require collecting at least 4^n data points to estimate the density matrix. For online QST, the measurement value at each sampling time can be combined into a measurement record sequence. Under the construction method of (7), the measurement record sequence b_k is composed of $[y_1, y_2, \dots, y_k]$, which is a dynamic sequence of data stream. However, from (7), we can observe that only one measurement value $\{y_k\}$ is related to the quantum state density matrix ρ_k at k -th sampling time, which is far from sufficient to reconstruct the density matrix ρ_k .

Therefore, at sampling time k , we derive the correspondence between the measurement record sequence $b_k = \{y_i\}_{i=1}^k$ and the quantum state ρ_k as shown in Table 1. Specifically, based on Table 1, we summarize the relationship between $b_k = \{y_i\}_{i=1}^k$ and ρ_k as:

$$y_i = \text{tr}(M_{k-i+1}^\dagger \rho_k) = \text{vec}(M_{k-i+1})^\dagger \text{vec}(\rho_k), \quad (8)$$

$$i = 1, \dots, k.$$

In order to make full use of the measurement record sequence and alleviate the computational burden in the online processing, a sliding window containing the most recent measurements is adopted in consideration. Therefore, we rewrite the measurement record sequence as:

$$b_k = \begin{cases} (y_1, \dots, y_{k-1}, y_k)^\text{T}, & k < l, \\ (y_{k-l+1}, \dots, y_{k-1}, y_k)^\text{T}, & k \geq l, \end{cases} \quad (9)$$

where l is the size of the sliding window.

When the number of obtained measurements is less than l , the size of the window is equal to the number of sampling times k . Otherwise, the size of sliding window remains l (containing the l most recent measurements). The update strategy of the sliding window is First-In-First-Out (FIFO), which allows the online stream of measurements to be incorporated into the model, while gradually removing old measurements.

Three points need to be emphasized here.

1) As can be seen from Table 1, the quantum state density matrix ρ_k can correlate with the measurement record sequence b_k by the relationship $[y_1, \dots, y_i, \dots, y_k] = [\text{tr}(M_k^\dagger \rho_k), \dots, \text{tr}(M_{k-i+1}^\dagger \rho_k), \dots, \text{tr}(M_1^\dagger \rho_k)]$, which enables us to use the measurement record sequence b_k to estimate the real-time quantum state ρ_k . With the increase of sampling times, the measurement information tends to be complete. This is why it is possible to reconstruct the quantum state density matrix that changes dynamically over time with one iteration.

2) Different with the construction method of measurement values in Heisenberg picture, where the online estimated state is always the unchanged initial state ρ_1 and then using the the system evolution model to obtain the estimated state $\hat{\rho}_k$ at the sampling time k [11, 12, 14, 15]. The proposed relationship construction in Table 1 avoids the requirement of evolution through the system evolution model after each estimation and enables real-time estimation of currently quantum states.

3) In fact, the corresponding relationship proposed in Table 1 is obtained without considering the dissipation of the quantum system model, so when we use it to estimate the real-time state with dissipation in the numerical simulation experiments of this paper, compared with the minimum measurement times under the guidance of compressed sensing theory, larger number of measurements is needed to achieve the desired accuracy.

According to Table 1, we construct the sampling matrix corresponding to (9) as:

$$\mathcal{A}_k = \begin{cases} (\text{vec}(M_k), \dots, \text{vec}(M_2), \text{vec}(M_1))^\dagger, & k < l, \\ (\text{vec}(M_l), \dots, \text{vec}(M_2), \text{vec}(M_1))^\dagger, & k \geq l. \end{cases} \quad (10)$$

It is worth noting that when the number of samplings is greater than or equal to l , the sampling matrix \mathcal{A}_k remains unchanged. At the same time, considering the measurement noise in the actual weak measurement process, using the sampling matrix \mathcal{A}_k and the density matrix ρ_k , we can rewrite b_k as $b_k = \mathcal{A}_k \text{vec}(\rho_k) + e_k$, where $e_k \in \mathbb{R}^k (l < k)$ or $e_k \in \mathbb{R}^l (k \geq l)$ is the measurement noise and is assumed to be Gaussian noise.

3 Online Optimization Algorithm with Measurement Noise

To minimize the measurement errors given the quantum constraints on density matrices, the online QST can be formulated as a convex optimization problem with constraints:

$$\begin{aligned} \min_{\hat{\rho}} \quad & \|\mathcal{A}_k \text{vec}(\hat{\rho}) - b_k\|_2^2 + (1/\eta_k) B_\theta(\hat{\rho}, \hat{\rho}_{k-1}), \\ \text{s.t.} \quad & \hat{\rho} \succeq 0, \text{tr}(\hat{\rho}) = 1, \hat{\rho}^\dagger = \hat{\rho}, \end{aligned} \quad (11)$$

where $\hat{\rho} \in \mathbb{C}^{d \times d}$ denotes the quantum state density matrix to be estimated; $\eta_k > 0$ is a learning rate parameter; convex set $\{\hat{\rho} \succeq 0, \text{tr}(\hat{\rho}) = 1, \hat{\rho}^\dagger = \hat{\rho}\}$ represents the quantum state constraints; $\text{tr}(X)$ denotes the sum of the diagonal elements of the matrix X ; $\|\mathcal{A}_k \text{vec}(\hat{\rho}) - b_k\|_2^2$ means to reduce the measurement error of the current estimated state; $B_\theta(\hat{\rho}, \hat{\rho}_{k-1})$ is the Bregman divergence [21], which reflects that the online estimation doesn't want to forget what has been learned too far; it is equal to the distance between the estimated state $\hat{\rho}$ at current sampling time k and the previous state estimation $\hat{\rho}_{k-1}$ under a smooth convex divergence function θ ($\nabla\theta$ denotes the first derivative of θ), defined as:

$$\begin{aligned} B_\theta(\hat{\rho}, \hat{\rho}_{k-1}) := & \theta(\text{vec}(\hat{\rho})) - \theta(\text{vec}(\hat{\rho}_{k-1})) - \\ & \text{vec}(\hat{\rho} - \hat{\rho}_{k-1})^\dagger \nabla\theta(\text{vec}(\hat{\rho}_{k-1})). \end{aligned} \quad (12)$$

The online alternating direction multiplier method (OADM) [20] is used to develop the online QST algorithm. For the constrained convex optimization problem

with separable two-objective variables, the basic idea of OADM is to decompose it into two sub-problems about the original variables. Then minimize the corresponding augmented Lagrangian functions of the two original variables in turn, and finally update the Lagrangian multiplier by dual gradient ascent. Furthermore, only one update is performed for the original variables and the Lagrange multiplier after each sampling.

In order to transform problem (11) into a two-objective optimization problem, we introduce the auxiliary variable \hat{e} . Hence, the online QST problem can be rewritten as:

$$\begin{aligned} \min_{\hat{\rho}, \hat{e}} \quad & (1/\eta_k) B_\theta(\hat{\rho}, \hat{\rho}_{k-1}) + I_C(\hat{\rho}) + (1/2\gamma) \|\hat{e}\|_2^2, \\ \text{s.t.} \quad & \mathcal{A}_k \text{vec}(\hat{\rho}) + \hat{e} = b_k, \end{aligned} \quad (13)$$

where $\gamma > 0$ is a regularization parameter; $I_C(\hat{\rho})$ is the indicator function; when the estimated state satisfies constraints $C := \{\hat{\rho} \succeq 0, \text{tr}(\hat{\rho}) = 1, \hat{\rho}^\dagger = \hat{\rho}\}$, $I_C(\hat{\rho})$ equals 0, otherwise $I_C(\hat{\rho})$ is ∞ .

The augmented Lagrangian of (13) is $L_k(\hat{\rho}, \hat{e}, \lambda) := I_C(\hat{\rho}) + (1/\eta_k) B_\theta(\hat{\rho}, \hat{\rho}_{k-1}) + (1/2\gamma) \|\hat{e}\|_2^2 - \langle \lambda, \mathcal{A}_k \text{vec}(\hat{\rho}) + \hat{e} - b_k \rangle + (\alpha/2) \|\mathcal{A}_k \text{vec}(\hat{\rho}) + \hat{e} - b_k\|_2^2$, where λ is the Lagrange multiplier and $\alpha > 0$ is the penalty parameter.

Based on the OADM routine, the online QST problem can be splitted into two small subproblems. Specifically, at the sampling time k , we first fix $\hat{e} \equiv \hat{e}_{k-1}$ and $\lambda \equiv \lambda_{k-1}$ to minimize $L_k(\hat{\rho}, \hat{e}_{k-1}, \lambda_{k-1})$ on the variable $\hat{\rho}$; then fix $\hat{\rho} \equiv \hat{\rho}_k$ and $\lambda \equiv \lambda_{k-1}$ to minimize $L_k(\hat{\rho}_k, \hat{e}, \lambda_{k-1})$ on the variable \hat{e} ; finally, the Lagrangian multiplier λ is updated by the dual gradient ascent method. Thus, in the OADM for online QST, the estimated density matrix $\hat{\rho}_k$, Gaussian noise \hat{e}_k , and the Lagrange multiplier λ_k are respectively:

$$\begin{cases} \hat{\rho}_k = \arg \min_{\hat{\rho}} \left\{ \frac{\alpha}{2} \|\mathcal{A}_k \text{vec}(\hat{\rho}) + \hat{e}_{k-1} - b_k - \lambda_{k-1}/\alpha\|_2^2 \right. \\ \quad \left. + I_C(\hat{\rho}) + (1/\eta_k) B_\theta(\hat{\rho}, \hat{\rho}_{k-1}) \right\}, & (14a) \\ \hat{e}_k = \arg \min_{\hat{e}} \left\{ (1/2\gamma) \|\hat{e}\|_2^2 \right. \\ \quad \left. + \frac{\alpha}{2} \|\mathcal{A}_k \text{vec}(\hat{\rho}_k) + \hat{e} - b_k - \lambda_{k-1}/\alpha\|_2^2 \right\}, & (14b) \\ \lambda_k = \lambda_{k-1} - \alpha (\mathcal{A}_k \text{vec}(\hat{\rho}_k) + \hat{e}_k - b_k). & (14c) \end{cases}$$

Note that index k represents the sampling times in which we apply the continuous measurement as well as the estimation updates. Therefore, only a single iteration is performed for (14) so as to devise a computationally minimalistic method suitable for real-time implementation. Since the Bregman divergence has diverse definitions [22], we can simplify the solution of the density matrix problem by defining an appropriate Bregman divergence term. In the following, we explicitly provide efficient methods for solving the two optimization problems for updating primal variables $\hat{\rho}, \hat{e}$ in (14a), (14b). The Lagrangian multiplier λ can be directly updated by (14c).

Subproblem of $\hat{\rho}_k$: we define the convex divergence function as a quadratic pseudo-norm $\theta(x) := (1/2) \|x\|_{P_k}^2 = x^\dagger (P_k/2)x$, where $x \in \mathbb{C}^{m \times 1}$ is the vector variables and $P_k \in \mathbb{C}^{m \times m}$ is any symmetric positive definite weight matrix. Bring $\theta(x)$

into (12), the Bregman divergence term in this case can be written as:

$$B_\theta(\hat{\rho}, \hat{\rho}_{k-1}) = (1/2) \|\text{vec}(\hat{\rho} - \hat{\rho}_{k-1})\|_{P_k}^2, \quad (15)$$

where we choose the weight matrix in the Bregman divergence term as

$$P_k = I - \alpha \eta_k \mathcal{A}_k^\dagger \mathcal{A}_k \succ 0. \quad (16)$$

More specifically, to ensure that P_k is positive definite, the learning rate η_k can be adaptively calculated as:

$$\eta_k = 1 / (\alpha \sigma_{\max}^2 + c), \quad (17)$$

where σ_{\max} is the largest singular value of \mathcal{A}_k (utilizing the random singular value decomposition, rsvd), $c > 0$ is a small constant. Moreover, from the definition of \mathcal{A}_k in (10), it holds that \mathcal{A}_k is a fixed matrix for $k \geq l$. As a result, the maximum singular value used for η_k needs only be computed l times (where l is the size of the window).

At this time, substituting (15) into the density matrix subproblem (14a) can cancel the quadratic term $(\alpha/2) \text{vec}(\hat{\rho})^\dagger \mathcal{A}_k^\dagger \mathcal{A}_k \text{vec}(\hat{\rho})$, which achieves the effect of performing a first-order linearization on the least square penalty term of the augmented Lagrangian at $\hat{\rho}_{k-1}$. Furthermore, the remaining Bregman divergence term after cancellation is $(1/2) \|\text{vec}(\hat{\rho} - \hat{\rho}_{k-1})\|_I^2$. Subsequently, the subproblem for $\hat{\rho}_k$ is equivalent to: $\arg \min_{\hat{\rho}} \{I_C(\hat{\rho}) + \langle \text{vec}(\hat{\rho} - \hat{\rho}_{k-1}), \alpha \mathcal{A}_k^\dagger (\mathcal{A}_k \text{vec}(\hat{\rho}_{k-1}) + \hat{e}_{k-1} - b_k - \lambda_{k-1}/\alpha) \rangle + \frac{1}{2\eta_k} \|\text{vec}(\hat{\rho} - \hat{\rho}_{k-1})\|_I^2\}$. Meanwhile, we let

$$\begin{aligned} \text{vec}(\tilde{\rho}_k) := & \text{vec}(\hat{\rho}_{k-1}) - \alpha \eta_k \mathcal{A}_k^\dagger (\mathcal{A}_k \text{vec}(\hat{\rho}_{k-1}) + \\ & \hat{e}_{k-1} - b_k - \lambda_{k-1}/\alpha), \end{aligned} \quad (18)$$

and merge the terms about $\text{vec}(\hat{\rho} - \hat{\rho}_{k-1})$ to get a concise density matrix subproblem as:

$$\begin{aligned} \hat{\rho}_k = & \arg \min_{\hat{\rho}} \|\text{vec}(\hat{\rho} - \tilde{\rho}_k)\|_I^2, \\ \text{s.t.} \quad & \hat{\rho} \succeq 0, \text{tr}(\hat{\rho}) = 1, \hat{\rho}^\dagger = \hat{\rho}. \end{aligned} \quad (19)$$

Using the Hermitian projection $(\tilde{\rho}_k + \tilde{\rho}_k^\dagger)/2$ to satisfy the constraint $\hat{\rho}^\dagger = \hat{\rho}$. Furthermore, since it is the calculation of the density matrix elements, (19) reduces to the density matrix projection problem [23]:

$$\begin{aligned} \hat{\rho}_k = & \arg \min_{\hat{\rho}} \|\hat{\rho} - (\tilde{\rho}_k + \tilde{\rho}_k^\dagger)/2\|_F^2, \\ \text{s.t.} \quad & \hat{\rho} \succeq 0, \text{tr}(\hat{\rho}) = 1, \end{aligned} \quad (20)$$

where $\|\cdot\|_F$ is the Frobenius norm.

Essentially, the problem of (20) is a nonlinear semidefinite programming problem and usually solved by interior-point method. Instead, we use a direct calculation method to solve it by the singular value decomposition. $(\tilde{\rho}_k + \tilde{\rho}_k^\dagger)/2$ can be diagonalized into $U\tilde{\Lambda}U^\dagger$ by unitary similarity, where $\tilde{\Lambda} = \text{diag}\{a_1, \dots, a_d\}$ is a diagonal matrix whose singular values are arranged in nonincreasing order; $U \in \mathbb{C}^{d \times d}$ is a unitary matrix. The optimal solution of (20) can be written as:

$$\hat{\rho}_k = U\hat{\Lambda}U^\dagger, \quad (21)$$

where $\hat{\Lambda} = \text{diag}\{x_1, \dots, x_d\}$ and $\{x_i\}_{i=1}^d$ are the singular values of the density matrix $\hat{\rho}_k$.

$\hat{\Lambda}$ is obtained from

$$\begin{aligned} \hat{\Lambda} &= \arg \min_{\Lambda} \|\Lambda - \tilde{\Lambda}\|_F^2, \\ \text{s.t.} \quad &\text{tr}(\Lambda) = 1, \Lambda \succeq 0, \end{aligned} \quad (22)$$

which exists the analytic solution as:

$$x_i = \max\{a_i - \kappa, 0\}, \forall i, \quad (23)$$

where κ is the solution of $\sum_{i=1}^d \max\{a_i - \kappa, 0\} = 1$.

Thus, we let $\kappa = a_i$, $i = 1, \dots, d$ determine the interval in which the optimal κ belongs. Assuming that $a_q - \kappa \geq 0$ and $a_{q+1} - \kappa < 0$ are established in $[a_q, a_{q+1}]$, the optimal κ can be calculated by $\sum_{i=1}^q (a_i - \kappa) = 1$ as:

$$\kappa = \left(\sum_{i=1}^q a_i - 1 \right) / q. \quad (24)$$

Subproblem of \hat{e}_k : (14b) is an unconstrained quadratic program that admits an analytical solution directly from first-order optimality condition of \hat{e} . Thus, \hat{e}_k is updated as:

$$\hat{e}_k = (\gamma\alpha / (1 + \gamma\alpha)) (\lambda_{k-1} / \alpha - \mathcal{A}_k \text{vec}(\hat{\rho}_k) + b_k). \quad (25)$$

The summary of the online QST-OADM algorithm proposed in this paper is shown in Algorithm 1.

Algorithm 1 QST-OADM

Require: Initial estimates $\hat{\rho}_0, \hat{e}_0 = 0, \lambda_0 = 0$; setting parameters $\alpha, \gamma > 0$; window size $l \in \mathbb{Z}_+$.

- 1: **for** $k = 1, 2, \dots$ **do**
 - 2: Obtain the measurement record sequence b_k ;
 - 3: Calculate the learning rate η_k according to (17);
 - 4: Calculate $\hat{\rho}_k$ according to (18);
 - 5: Run singular value decomposition on $(\hat{\rho}_k + \hat{\rho}_k^\dagger) / 2$ as $U \text{diag}\{a_i\} U^\dagger$;
 - 6: Calculate singular values $\text{diag}\{x_i\}$ of $\hat{\rho}_k$ according to (23) and (24);
 - 7: Update $\hat{\rho}_k$ according to (21);
 - 8: Update \hat{e}_k according to (25);
 - 9: Update λ_k according to (14c);
 - 10: **end for**
-

Remarks:

1) Compared with the offline QST algorithms [4,5] (both the measurement values b and the sampling matrix \mathcal{A} are all fixed for an invariant quantum state ρ), that need to pass the same set of measurement data through multiple iterations to estimate a fixed quantum state, the QST-OADM algorithm proposed in this paper focuses on the general dynamic state and obtains the estimated state $\hat{\rho}_k$ in only one iteration, which provides a naturally *online* tracking protocol for real-time applications. Moreover, a key difference between online and offline QST is the Bregman divergence

$B_\theta(\hat{\rho}, \hat{\rho}_{k-1})$ in (11) that calculates the distance between the current state to be estimated and the previous state estimation. It is the core embodiment of the tracking ability of the QST-OADM.

2) Combining the online alternating direction multiplier method for simultaneous estimation of the quantum state ρ_k and measurement noise e_k is novel in online QST. Compared with ML [11], LS [15] (ML and LS are essentially offline algorithms), QST-OADM can explicitly solve the online QST problem without running iteratively for every sampling. In terms of MEG [13], both QST-OADM and MEG use the first-order information of quantum state density matrix problem, the main difference is that the learning rate of QST-OADM can be adaptively adjusted at every estimation, which can achieve fast and high-precision state tracking. The QST-OADM avoids pseudo-inverse operation of LS solution for the quantum state subproblem whose calculation complexity is $\mathcal{O}(d^6)$. The computational complexity of ML is $\mathcal{O}(d^4)$. Similar to MEG, the main computational complexity for each estimation of QST-OADM is $\mathcal{O}(d^3)$, which is the cost for singular value decomposition required for updating the density matrix.

4 Numerical Simulation Experiments

In this section, three numerical simulation experiments are carried out. The first and second experiments use the proposed QST-OADM algorithm to explore the impacts of the external control strength u_x and the sliding window size l on the reconstruction performance of online QST, respectively. The online processing properties of the proposed QST-OADM, comparing with maximum likelihood estimation (ML) [11], matrix exponential gradient (MEG) [13], and least squares (LS) [15] are illustrated in the third experiment.

In the experiments, the true quantum state ρ_k of the estimated system S is generated by (5). The measurement value y_i at each sampling time is generated by (7). The measurement record sequence is constructed by (9). The corresponding sampling matrix \mathcal{A}_k is defined by (10). The initial state density matrix of the true n -qubit system is chosen as $\rho_1^n = \underbrace{\rho_1 \otimes \dots \otimes \rho_1}_n$, $\rho_1 = [0.5, (1-i)/(\sqrt{8}); (1+i)/(\sqrt{8}), 0.5]$,

and the initial estimate is selected as $\hat{\rho}_1^n = \underbrace{\hat{\rho}_1 \otimes \dots \otimes \hat{\rho}_1}_n$, $\hat{\rho}_1 = [0, 0; 0, 1]$. The initial measurement operator is $M_1^n = \underbrace{\sigma_z \otimes \dots \otimes \sigma_z}_n$ (in all cases we use the superscript n to

indicate the number of qubits, ranging in $\{1, 2, 3, 4\}$ in our experiments). In the weak measurement operators of a two-level quantum system, $L_1 = \xi \sigma_z$, $H_1 = \sigma_z + u_x \sigma_x$, which are defined in (2). The measure efficiency η and the interaction strength ξ are set to 0.5 and 0.07, respectively. The amplitude of the system stochastic noise dW is 0.001. The signal-to-noise ratio (SNR) of the Gaussian measurement noise e is 30dB. The parameters involved in QST-OADM are set as follows: the penalty parameter $\alpha = 5n$, $\gamma = 0.1$, and the learning rate η_k can be adaptively determined by (17). For the different comparison algorithms ML, LS, and MEG, we reimplement them on the same quantum system, and each algorithm is adjusted to its best performance.

Specifically, for MEG with manual learning rate, for 1, 2, 3, and 4-qubit systems, the learning rate is tuned to 0.28, 0.33, 0.33, and 0.35, respectively. All simulations are conducted in MATLAB R2016a, running in Inter Core i7-8750M CPU, clocked at 2.2GHz, with a memory of 16GB.

As for the real-time true state ρ_k which is in the free-evolution and evolves to the maximum mixed state gradually. The performance of the estimated state $\hat{\rho}_k$ is evaluated by the fidelity based on Schatten's 2-norm, defined as [24]

$$F_1(\rho_k, \hat{\rho}_k) := \frac{\text{tr}(\rho_k \hat{\rho}_k)}{\max\{\text{tr}(\hat{\rho}_k^2), \text{tr}(\rho_k^2)\}}, \quad (26)$$

where $\text{tr}(\rho^2)$ represents the degree of mixing of the quantum state ρ , also named purity.

The range of fidelity is [0,1]. The closer to 1, the more similar the estimated state and the true state are. The process from pure state dissipation to the maximum mixed state corresponds to the decrease of purity from 1 to $1/d$ ($d = 2^n$). In addition, it is noteworthy that in most cases [3–5, 9–11, 13–16, 18], the fidelity is defined as $F_2(\rho_k, \hat{\rho}_k) := \text{tr}(\sqrt{\sqrt{\hat{\rho}_k} \rho_k \sqrt{\hat{\rho}_k}})$ [25]. At the same time, there are some other definitions of fidelity, such as the superfidelity, defined as $F_3(\rho_k, \hat{\rho}_k) := \text{tr}(\rho_k \hat{\rho}_k) + \sqrt{1 - \text{tr}(\rho_k^2)} \sqrt{1 - \text{tr}(\hat{\rho}_k^2)}$ [26]; the A-fidelity, defined as $F_4(\rho_k, \hat{\rho}_k) := (\text{tr}(\sqrt{\rho_k} \sqrt{\hat{\rho}_k}))^2$ [27]; and the geometric mean fidelity, defined as $F_5(\rho_k, \hat{\rho}_k) := \text{tr}(\rho_k \hat{\rho}_k) / \sqrt{\text{tr}(\hat{\rho}_k^2) \text{tr}(\rho_k^2)}$ [28]. We will show in subsection 4.1 that (26) is more suitable for measuring the similarity of mixed states of open quantum systems.

4.1 Impact of the External Control Strength on Online QST

In this simulation experiment, we mainly test the impact of online QST with or without the external control strength u_x . In order to intuitively reflect the estimation results, we choose the 1-qubit system, whose evolution trajectory can be clearly drawn on a Bloch sphere. For online QST, the number of sampling times is set to $N = 100$. The size of the sliding window is selected as $l = 16$, which is shown to be sufficient to reconstruct the density matrix of 1-qubit system.

Fig. 2 depicts that:

1) When $u_x = 0$, from Fig. 2(a), the online estimation of quantum states cannot be realized. The reason is that the trajectory of the true state is parallel to the $x-y$ plane and coincides with the initial measurement operator M_1 , which results in the inability to measure sufficient effective information of the system. In contrast, when a non-zero external control strength $u_x = 2$ is applied, from Fig. 2(b), we observe that QST-OADM can achieve stable state tracking after 9 samplings, which indicates the external control strength is necessary for online QST.

2) The estimated state (blue) trajectory is consistent with the true state only when the true state at the maximum mixed state (purity = 0.50) in Fig. 2(a). However, from Fig. 2(c), for the purity when the accuracy of fidelity exceeds 90% (as a baseline), F_1 is 0.56; F_2 is 0.81; F_3 and F_4 are 0.68; and F_5 is 0.62. F_1 is the closest to the actual

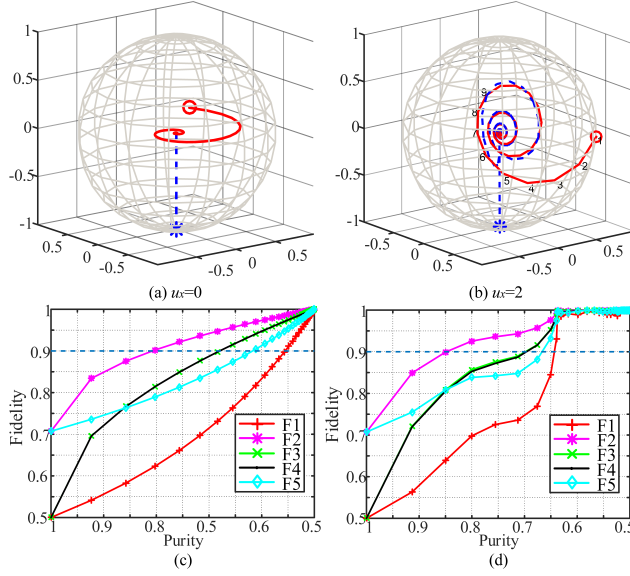


Fig. 2 (a) and (b) are the online estimation results with $u_x = 0$ and $u_x = 2$. The red solid line and the blue dashed line in the Bloch sphere are the true state trajectory and estimated state trajectory by QST-OADM, respectively. The red circle and the blue star represent the initial values of true and estimated states, respectively. The number on the trajectory in the Bloch sphere of (b) denotes the sampling times. (c) and (d) correspond to the performance evaluation of the $F_1 - F_5$ fidelity in the case of $u_x = 0$ and $u_x = 2$, respectively. The x-axis and y-axis represent the purity change process of true state and the fidelity of the estimated state at each sampling time, respectively.

situations. From Fig. 2(d), among $F_1 - F_5$, the performance evaluation of F_1 is more sensitive and only F_1 achieves more than 90% fidelity in the ninth sampling. Thus, it can be concluded that F_1 gives a more precise and suitable evaluation performance.

4.2 Impact of the Sliding Window Size on Online QST

In this experiment, for 1, 2, 3, and 4-qubit systems, we compare the impact of different sliding window sizes on online QST performance. The external control strength is $u_x = 2$. The number of sampling times is set to $N = 500$. The size of the sliding window is taken as $l = 1, \dots, 100$. At each window size, the comparison criterion is the minimum number of sampling times k_{min} (or estimations) required to achieve more than 90% fidelity. The k_{min} is expected to be smaller, indicating that the dynamic state can be tracked with fewer samplings.

Fig. 3 depicts that as the size of the sliding window increases, the minimum number of sampling times k_{min} gradually decreases and stabilizes after the sliding window reaches a certain size. It means that there is a proper sliding window size l^* for online QST of different number of qubits. For online estimation of 1, 2, 3, and 4-qubit systems, the proper l^* could be 8, 13, 16, and 75, respectively.

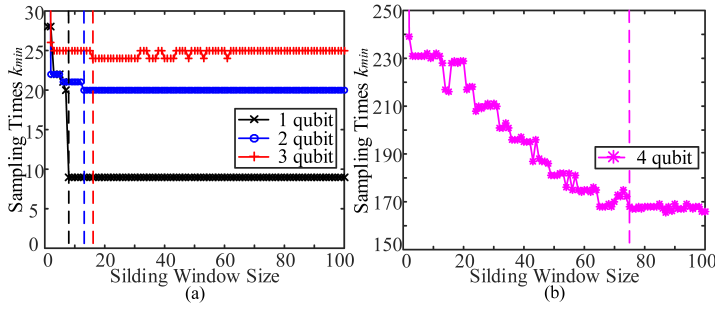


Fig. 3 Impact of the sliding window size on online estimation. Black, blue, red and pink dashed lines represent where the proper window sizes for the 1, 2, 3, and 4-qubit systems are, respectively.

4.3 Online Processing Properties of QST-OADM, LS, ML, and MEG

In order to verify the online processing performance, we compare the proposed QST-OADM with three existing algorithms (LS, ML, and MEG) in online QST of 1, 2, 3, and 4-qubit systems. As we have mentioned in Section 1, since Yang's CVX-LS algorithm [15] requires multiple iterations for each sampling time, which is time-consuming for online processing, it will not be compared in this paper. As an alternative, we first resort to the pseudo-inverse command *pinv* in MATLAB to get the solution of least squares by ignoring the quantum state constraints, and then obtain the estimation $\hat{\rho}_k$ that satisfies the constraints using projection (20). In ML for online QST [11], the ML-estimator is set to execute a single run at each estimation. The ML-estimator can not ensure that the estimated state satisfies is optimal by directly setting the negative eigenvalue of the estimated state to 0 and trace normalization for meeting the physical constraints. MEG [13] guarantees the positive semidefinite of the density matrix through exponential operations. Based on experiments in subsection 4.1 and 4.2, for 1, 2, 3, and 4-qubit systems, the size of the sliding window is set to 8, 13, 16, and 75, respectively. The external control strength u_x equals 2 and the number of sampling times N equals 500.

Fig. 4 depicts the fidelity with respect to the number of samplings in the online estimation process. One can see that, for 1, 2, 3, and 4-qubit systems, the number of sampling times required for different algorithms to reach more than 90% fidelity is QST-OADM (9, 19, 25, 168), LS (17, 21, 28, 256), ML (16, 22, 30, 262), and MEG (10, 21, 29, 206), respectively, which shows that the proposed QST-OADM has the lowest sampling times among the 4 algorithms.

We also compare the fidelity of different algorithms for a 4-qubit system running 200 times, which are 92.06% (QST-OADM), 81.86% (LS), 87.01% (ML), and 88.88% (MEG), respectively. Under the same sampling times, the estimation accuracy of QST-OADM is higher than the accuracy of LS, ML, and MEG algorithms.

Fig. 5 further explicitly shows the average running time of the 4 algorithms at each sampling time. From Fig. 5 it indicates that the proposed QST-OADM algorithm is the most efficient algorithm in the comparison. When $n=1, 2, 3,$ and 4 , the estimated time required for QST-OADM is 0.0540s, 0.0616s, 0.0757s and 0.2061s respectively. Moreover, as the number of qubits increases, the online processing advantages of

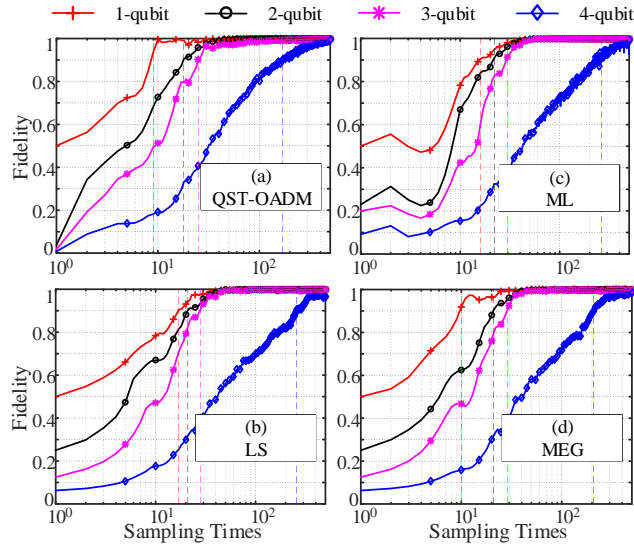


Fig. 4 Comparisons of online quantum state reconstruction performances using QST-OADM, LS, ML, and MEG algorithms are shown in (a), (b), (c), and (d), respectively. The solid lines with plus, circle, star and diamond marks represent the 1, 2, 3, and 4-qubit systems, respectively. The dashed lines of red, black, pink, and blue indicate the number of sampling times when the estimated states first reach more than 90% fidelity, respectively.

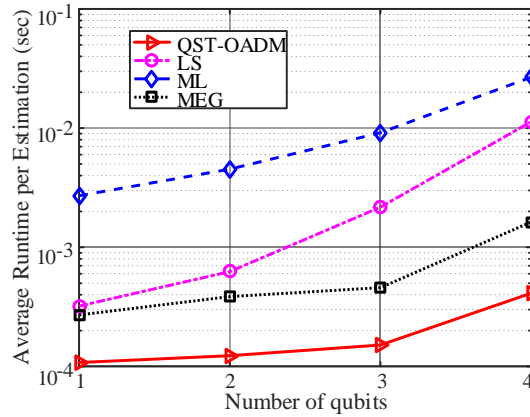


Fig. 5 Comparison of average running time for each estimation of QST-OADM, LS, ML, and MEG algorithms.

QST-OADM become even larger. For a 4-qubit system, the average running time of QST-OADM, LS, ML, and MEG is $4.12e-4s$, $1.13e-2s$, $2.68e-2s$, and $1.60e-3s$, respectively. The merit of the proposed algorithm is that it can track the dynamic quantum state fast and efficiently, which embodies its superiority in online QST.

5 Conclusion

In this paper, a real-time online algorithm QST-OADM with measurement noise was developed, which required only one iteration at each sampling time. Furthermore, for achieving high estimation accuracy and improving efficiency, the sliding window of measurements and adaptive learning rate were adopted. The algorithm we proposed was efficient and fast to estimate the real-time quantum state. Numerous simulation experiments demonstrated the superiority of the potential merits of the method as a real-time solution for state tomography in multi-qubit quantum systems.

References

1. Paris, M., Rehacek, J.: quantum state tomography. Springer Science & Business Media (2004)
2. Kalev, A., Hen, I.: Fidelity-optimized quantum state tomography. *New J. Phys.* 17, 093008 (2015)
3. Gross, D., Liu, Y., Flammia, S.T.: Quantum state tomography via compressed sensing. *Phys. Rev. A.* 105, 150401 (2010)
4. Zhang, J., Cong, S., Ling, Q., Li, K.: An efficient and fast quantum state estimator with sparse disturbance. *IEEE transactions on cybernetics.* 49, 2546–2555 (2018)
5. Li, K., Zheng, K., Yang, J., Cong, S., Liu, X., Li, Z.: Hybrid reconstruction of quantum density matrix: when low-rank meets sparsity. *Quantum Inf. Process.* 16(12), 299 (2017)
6. Shalevshwartz, S.: Online learning and online convex optimization. *Foundations and Trends in Machine learning.* 4, 107-194 (2012)
7. Hesterberg, T.: Introduction to stochastic search and optimization: estimation, simulation, and control. *Journal of the American Statistical Association.* 46, 368-369 (2012)
8. Li, K., Zhang, H., Kuang, S., Meng, F., Cong, S.: An improved robust ADMM algorithm for quantum state tomography. *Quantum Inf. Process.* 15(6), 2343-2358 (2016)
9. Leghtas, Z., Mirrahimi, M., Rouchon, P.: Back and forth nudging for quantum state tomography by continuous weak measurement. *Proceedings of the 2011 American Control Conference.* 4334-4339 (2011). doi:10.1109/ACC.2011.5991108
10. Wang, L., Zhou, Y. Y., Zhou, X. J., Chen, X., Zhang, Z.: Erratum: Correction to: New scheme for measurement-device-independent quantum key distribution. *Quantum Inf. Process.* 18, (2019)
11. Silberfarb, A., Jessen, P.S., Deutsch, I.H.: Quantum state reconstruction via continuous measurement. *Phys. Rev. A.* 95, 030402 (2005)
12. Smith, G.A., Silberfarb, A., Deutsch, I.H., Jessen, P.S.: Efficient quantum-state estimation by continuous weak measurement and dynamical control. *Phys. Rev. L.* 97, 180403 (2006)
13. Youssry, A., Ferrie, C., Tomamichel, M.: Efficient online quantum state tomography using a matrix-exponentiated gradient method. *New J. Phys.* 21, 033006 (2019)
14. Ralph, J., Jacobs, K., Hill, C.D.: Frequency tracking and parameter estimation for robust quantum state tomography. *Phys. Rev. A.* 84, 052119 (2011)
15. Yang, J., Cong, S., Kuang, S.: Real-time quantum state tomography based on continuous weak measurement and compressed sensing. *Proceedings of the International MultiConference of Engineers and Computer Scientists.* 2, 499-504 (2018)
16. Cong, S., Tang, Y., Sajede, H., Li, K., Yang, J.: On-line quantum state tomography using continuous weak measurement and compressed sensing. *Science China Inf. Sci.* 62, 1-4 (2019)
17. Grant, M., Boyd, S., Ye, Y.: CVX: Matlab software for disciplined convex programming. (2008)
18. Harraz, S., Cong, S.: State transfer via on-line state estimation and Lyapunov-based feedback control for a n-Qubit system. *Entropy.* 21, 751-762 (2019)
19. Hong, T., Zhu, Z.: Online learning sensing matrix and sparsifying dictionary simultaneously for compressive sensing. *Signal Processing.* 153, 188-196 (2018)
20. Wang, H., Banerjee, A.: Online alternating direction method. *29th International Conference on Machine Learning, ICML.* 1119–1126 (2012)
21. Zhang, J.: Divergence function, duality, and convex analysis. *Neural Computation.* 16, 159-195 (2004)
22. Goh, G., Dey, D.: Bayesian model diagnostics using functional Bregman divergence. *Journal of Multivariate Analysis.* 124, 371–383 (2014)

23. Gonalves, D.S., Gomes-Ruggiero, M.A., Lavor, C.: A projected gradient method for optimization over density matrices. *Optimization Methods and Software*. 31, 328-341 (2016)
24. Liang, Y.C., Yeh, Y.H., Mendona, P.E., Teh, R.Y., Reid, M.D., Drummond, P.D.: Quantum fidelity measures for mixed states. *Reports on Progress in Physics*. 82, 076001 (2019)
25. Yamamoto, N., Mikami, T.: Entanglement-assisted quantum feedback control. *Quantum Inf. Process.* 16, 179 (2017)
26. Gilchrist, A., Langford, N.K., Nielsen, M.A. Distance measures to compare real and ideal quantum processes. *Phys. Rev. A*. 71, 062310 (2005)
27. Ma, Z., Zhang, F., Chen, J.: Geometric interpretation for the A fidelity and its relation with the Bures fidelity. *Phys. Rev. A*. 78, 064305 (2008)
28. Wang, X., Yu, C., Yi, X.: An alternative quantum fidelity for mixed states of qudits. *Phys. Rev. A*. 373, 58-60 (2008)